ANDROLOGY (Special Issue on The Clinic and Biology of the Epididymis)

Epididymal mRNA expression profiles for the protein disulfide isomerase gene family: modulation by development and androgens

Samuel G Fernandes[1], Lucas G A Ferreira[1], Adam M Benham[2], Maria Christina W Avellar[1],*

[1]Department of Pharmacology, Universidade Federal de São Paulo – Escola Paulista de Medicina, São Paulo, SP, 04044-020, Brazil; [2]Department of Biosciences, Durham University, Stockton Road, Durham, DH1 3LE, UK.

LE

*Corresponding Author: Laboratory of Molecular, Endocrine and Reproductive Pharmacology, Department of Pharmacology, Universidade Federal de São Paulo – Escola Paulista de Medicina, Rua Três de maio, 100, São Paulo, SP, 04044-020, Brazil; E-mail address: avellar@unifesp.br

Email addresses:
samuelguilerme@gmail.com
lucasgaaferreira@gmail.com
adam.benham@durham.ac.uk
avellar@unifesp.br

Keywords: protein disulfide isomerase, androgens, epididymis, development, endoplasmic reticulum, protein quality.

Highlights

- Transcriptional profile of *Pdi* genes have been examined in the developing epididymis.
- *Pdi* gene expression was differentially regulated during epididymal morphogenesis and along postnatal life.
- Surgical castration downregulated *Pdi* genes in adult rat epididymis.
- *In silico* analysis revealed the *PDI* transcriptional profile along human epididymis.

ABSTRACT

Background The endoplasmic reticulum is the central hub for protein quality control, where the protein disulfide isomerases (PDIs), encoded by at least 21 genes, play a pivotal role. These multifunctional proteins contribute to disulfide bond formation, proper folding, and protein modifications, and may act as hormone-binding proteins (e.g., steroids), influencing hormone biology. The interplay between ER proteostasis, PDIs, and epididymis - a crucial site for sperm maturation - remains largely understudied.

Objectives This study characterizes transcriptional signatures of *Pdi* genes in the epididymis.

Material and methods Transcriptional profiles of selected *Pdi* genes were assessed in adult Wistar rat tissues, and epididymis under different experimental conditions (developmental stages, surgical castration, and efferent ductules ligation, EDL). *In silico* bioinformatic analyses identified expression trends of this gene family in human epididymal segments.

Results *Pdia6*, *Pdia3*, *Erp44, P4hb*, *Pdia5*, *Erp29*, and *Casq1* transcripts were detected in both reproductive and non-reproductive tissues, while *Casq2* exhibited higher abundance in vas deferens, prostate and heart. *Pdilt*, highly expressed in testis, and *Pdia2*, highly expressed in heart, showed minimal mRNA levels in the epididymis. In the mesonephric duct, epididymal embryonic precursor, *P4hb*, *Pdia3*, *Pdia5*, *Pdia6* and *Erp29* mRNAs were found at gestational day GD17.5. Except for *Erp29,* which remained stable, these *Pdi* transcript levels increased from GD17.5 to GD20.5, when epididymal morphogenesis occurs, and were maintained to varying degrees in the epididymis during postnatal development. Surgical castration downregulated *P4hb*, *Pdia3*, *Pdia5*, *Pdia6*, and *Erp29* transcripts, an effect reversed by testosterone replacement. Conversely, transcript levels remained unaffected by EDL, except *P4hb,* which was reduced in caput epididymis. All 21 *PDI* genes exhibited diverse transcriptional profiles across the human epididymis.

Discussion and conclusion The findings lay the foundations to explore *Pdi* genes in epididymal biology. As a considerable proportion of male infertility cases are idiopathic, targeting hormonal regulation of protein quality control in epididymis represents a route to address male infertility and advance therapeutic interventions in this domain.

1 INTRODUCTION

After production in the testis, spermatozoa reach the epididymis via the efferent ductules. The epididymal tissue is a single long and highly convoluted tubule divided into four regions - the initial segment, caput, corpus, and cauda - which concentrates, transports, protects and facilitates maturation of spermatozoa prior to their storage in the caudal compartment. The septa within each region further subdivide the epididymis into intra-segmental regions (10 in mouse, 19 in rat, 8 in human). [1–3] Each segment is composed of its respective distinct epithelial cells that exhibit diverse patterns of gene expression and absorptive/secretory activities of proteins and other factors; these cellular activities shape unique luminal microenvironments sequentially established along the tissue that is crucial for sperm maturation and fertilizing ability. [1, 4]

The development of the epididymis from its embryonic precursor, the mesonephric ducts (also called Wolffian duct, WD) to a mature and functional adult tissue is primarily orchestrated by androgens acting via the androgen receptor (AR; encoded by the *NR3C4* gene), alongside other endocrine, paracrine, lumicrine and immunological factors. [1] At birth, the epididymis remains immature, with epithelial cell development and differentiation progressing until puberty. Luminal testicular factors that reach the proximal epididymis via efferent ductules further contribute to completing differentiation of the epithelium. Throughout the epididymis, various epithelial cell types - together with nearby immune cells - establish, maintain and regulate the blood-epididymal barrier, orchestrating a unique luminal milieu that supports sperm transport, maturation, and protection from metabolic stress and injury (both infectious and non-infectious), and ensures selective tolerance to autoantigenic spermatozoa. Given its role in sperm maturation (i.e., the progressive acquisition of sperm motility and fertilizing capacity), the epididymis is therefore indispensable for functional male fertility. [1, 5]

During sperm maturation, spermatozoa undergo continuous remodeling of their membrane surface organization, and in their protein, lipid and RNA profiles. This process depends on the coordinated attachment and shedding of molecules, primarily regulated by proteins synthesized in the epididymis and subsequently secreted into its lumen by the epithelial cells, where they interact with the sperm directly or via extracellular vesicles (i.e., epididymosomes). [1,6] To “interface” effectively with epididymal tissue and maturing spermatozoa, newly synthesized proteins must undergo essential post-translational modifications - folding, oligomerization, disulfide

bond formation, N-linked glycosylation, and cleavage of the N-terminal signal peptides for those in the secretory pathway. [1, 6] The quality control of proteins synthesized and secreted by the epithelium into the epididymal lumen remains not fully understood.

The endoplasmic reticulum (ER) plays a vital role in controlling protein quality to designated sites both inside and outside the cell, while also ensuring overall physiological homeostasis, including redox status and calcium regulation. Disruption of the ER can lead to diseases related to protein folding and lipid metabolism, underscoring its importance in cell health. [7, 8] In the human epididymis, the ER within epithelial principal cells occupies a notably large area (~40 μm^2), indicative of its heightened activity. [9] Given the high secretory demands of the epididymal epithelium, robust protein folding and quality control mechanisms are essential, highlighting the relevance of ER chaperone protein families in this tissue. Among these, the protein disulfide isomerase (PDI) family, part of the thioredoxin superfamily of redox proteins, are at the forefront of supporting protein quality in the ER by serving as both oxidoreductases and multifunctional molecular chaperones. Investigating the expression patterns and androgen dependence of *Pdi* genes may provide valuable insights into epididymal biology and male reproductive health. As there are at least 21 PDI genes in mammals (**Fig.S1)** [10, 11] uncovering their expression profile in relation to the developing epididymis and dependence on androgens can provide insights into their roles within this tissue.

As a folding catalyst, PDIs guide the formation, isomerization and rearrangement of disulfide bonds both within and between protein subunits, thus preventing the aggregation of misfolded proteins. [7, 12] P4HB (PDI or PDIA1), the prototypical member, has a four-domain structure with thioredoxin-like domains (a, b, b' and a') connected by an X-linker (bridging b' and a') and a functional C-terminal ER retention sequence. Other PDIs differ in redox activity (e.g., PDILT), or in the a and b domains arrangements (e.g., PDIA5 and PDIA6), while some PDIs contain only a-type (transmembrane subfamily TMX1, 2 and 4 and the AGR subfamily) or b-type domains (**Fig.S1).** [10, 11] PDIs can reside in other cellular compartments, be secreted into the extracellular environment, and are found in both plasma and seminal fluid. [13, 14] Consequently, they can influence a wide range of biological processes, including the control of cell survival and death. [7, 15] PDIs can also bind and influence the bioavailability of hormones (T3: e.g., P4HB, Erp29 [16]; estrogens: P4HB, PDIA2 [17-19]), assist estrogen receptor

signaling as molecular chaperones (ERS1; e.g., PDIA2 [18]), and act as membrane receptor for steroid signaling (e.g., 1,25-hydroxyvitamin D3; PDIA3 [20, 22]). However, a number of PDIs still await comprehensive functional studies.

Here, we investigated the transcriptional profile of *Pdi* genes during prenatal and postnatal development of the rat epididymis, and in the epididymis of adult rats subjected to surgical castration and efferent ductules ligation (EDL) to assess, respectively, the influence of androgens and testicular factors on these profiles. Using *in silico* analyzes, we mapped the transcriptional profile of *PDI* genes expressed in the human epididymis. Overall, our results establish a molecular foundation for multiple PDI transcripts in the developing and adult epididymis, and uncovered those responsive to androgen regulation, lending support to future studies that target PDI gene and protein expression to epididymal function.

2 MATERIALS AND METHODS

2.1 Animals

Male and female Wistar rats (*Rattus norvegicus* albino) were bred and housed in the animal facility of the Instituto Nacional de Farmacologia e Biologia Molecular (INFAR), Universidade Federal de São Paulo - Escola Paulista de Medicina (UNIFESP-EPM) under controlled light (12 h light/dark cycle) and temperature (22 - 25°C) with free access to food and water (*ad libitum*). To achieve timed mating, a single male rat was housed overnight with two female rats. Copulation was confirmed the next morning by the presence of spermatozoa in vaginal smears, and the time point was defined as gestational day (GD) 0.5 of the pregnant rat. [22, 23] Male rat fetuses at GD17.5 and GD20.5, and at postnatal day (PND) 1, PND5, PND10, PND20, PND40, PND90 and PND120 were used. Male neonatal rats at PND1 and PND5 were anesthetized by hypothermia prior to euthanasia by decapitation. Surgical procedures (castration and efferent ductules ligation, EDL) were performed with rats anesthetized with ketamine/xylazine cocktail (86.7 mg/kg and 8.7 mg/kg of body mass, respectively; i.p.). Euthanasia of dams and males at different PNDs was performed with an inhaled overdose of isoflurane (Cristália, SP, Brazil), followed by bilateral pneumothorax. All animal manipulations were performed in accordance with the National Institutes of

Health Guide for the Care and Use of Laboratory Animals and approved by the Research Ethical Committee of UNIFESP-EPM (CEUA, #5908210916).

2.2 Animal experimental procedures and tissue harvesting

After euthanasia, fetuses were removed from the dams by laparoscopy and immediately placed in ice-cold DPBS (Thermo Fisher Scientific, NY, USA) before decapitation. Male fetuses were identified by inspection of the gonads at GD17.5 and urogenital distance at GD 20.5. Mesonephric ducts were dissected under stereomicroscopy, immediately frozen in liquid nitrogen, and stored at -75ºC until use. The mesonephric ducts of male fetuses at GD17.5 (uncoiled duct) and GD20.5 (coiled duct) were harvested considering the time window when male fetal plasma testosterone increases and epididymal morphogenesis occurs. [5, 23] Male rats were euthanized at different postnatal time points, being neonates (PND1, PND5 and PND10), sexually immature (PND20 and PND40) and mature rats (PND90 or PND120), as previously reported. [23,24] Epididymides were harvested immediately and dissected as whole tissue (PND1-PND20) or into three parts, i.e., caput (including the initial segment), corpus, and cauda epididymis (PND40, PND90, and PND120). Reproductive tissues (testis, vas deferens, seminal vesicle, and ventral prostate) and nonreproductive tissues (kidney, adrenal gland, lung, liver, skeletal muscle and heart) were also collected from PND120 rats. All tissue samples were immediately frozen in liquid nitrogen and stored at -75ºC until use.

2.3 Bilateral surgical castration and testosterone replacement

Male adult rats (PND90) were sham-operated (control; CTL) or castrated as previously described. [25] The rats were euthanized 7 (7d) or 15 days (15d) after surgical procedures. An additional group of 7-day castrated rats was treated with testosterone propionate (1 mg/kg of body mass, s.c.) for 6 consecutive days and euthanized 15 days after surgery (7dT). Caput (including the initial segment), corpus and cauda epididymis were harvested and immediately frozen in liquid nitrogen and stored at -75ºC. The body mass and the mass (absolute and relative) of the reproductive tissues (seminal vesicle, vas deferens and ventral prostate) were used to measure the efficacy of surgical castration and testosterone treatment in the animals. The relative mass of the epididymis and reproductive

tract tissues was consistent with previously reported data [25], indicating the successful establishment of this castration model.

2.4 Bilateral ligation of the efferent ductules

Male adult rats (PND90) were sham-operated (control) or submitted to efferent ductules ligation (EDL) as previously described.[16, 27] The rats were euthanized 15 days after surgical procedures. The epididymides were harvested, dissected and divided into regions (initial segment and caput), which were then immediately frozen in liquid nitrogen and stored at -75ºC until use.

2.5 Total RNA extraction and complementary DNA (cDNA) synthesis

Frozen tissue samples (~20-30 mg) were minced in liquid nitrogen and used for total RNA extraction using the TRIzol™ reagent (Thermo Fisher Scientific, California, USA) or PicoPure™ RNA Isolation kit (for mesonephric ducts; one pair mesonephric ducts per sample; Thermo Fisher Scientific). Reverse transcriptase reactions were performed with either 0.5 µg (mesonephric ducts) or 2.5 µg (epididymis and other tissues) of total RNA and 2.5 µM oligo-(dT) in a total volume of 10 µl, according to the manufacturer's instructions (Thermoscript RT-PCR system). A negative control (without reverse transcriptase) was routinely performed to exclude contamination with genomic DNA. The produced cDNAs were either used immediately or stored at -20°C until use.

2.6 Reverse transcriptase and polymerase chain reaction (RT-PCR)

RT-PCR (semi-quantitative) or RT-qPCR (real time quantitative PCR analysis) was performed as previously described. [22] Oligonucleotide pairs (**Table S1**) used for amplification of each target genes were designed using the NCBI/Primer Blast tool (https://www.ncbi.nlm.nih.gov/tools/primer-blast) and purchased commercially from Exxtend Biotechnology (Campinas, SP, Brazil).

Semi-quantitative PCR assays were performed with PCR buffer (20 mM Tris-HCl pH 8.4; 50 mM KCl), $MgCl_2$ (1.5 mM), dNTPs mixture (0.2 mM), Taq DNA polymerase (2 U), 0.4 µM of each oligonucleotide pair

(sense and antisense) and cDNA (final concentration of 12.5 ng/µl). Reactions were performed under the cycling conditions of 35 cycles of 1 min at 95 °C, 1 min at 60 °C and 1.5 min at 72°C. Negative controls were performed in the absence of cDNA. The expression levels of the glyceraldehyde 3-phosphate dehydrogenase gene (*Gapdh*) were used as an endogenous control. Amplicons (*Pdia2*, *Pdia5*, *Pdia6*, *Pdilt*, *Erp29*, *Erp44*, and *Casq2*) were gel purified (QIAquick PCR Purification kit, Qiagen) and subjected to automated DNA sequencing (ABI PRISM 377, Applied Biosystems, USA). The resulting nucleotide sequences were confirmed by BLAST in the NCBI database (https://www.ncbi.nlm.nih.gov/blast).

Quantitative PCR (qPCR) was performed with SYBR Green Master Mix kit (Kapa Biosystems, Cape Town, South Africa) using the ABI PRISM 7500 Sequence Detection System. Amplifications were performed with 25 to 100 nM of each oligonucleotide pair (**Table S1**) and cDNA (final concentration of 0.5 ng/µl for mesonephric duct; 0.5 ng/µL for whole epididymis, PND1-PND20; 0.5 ng/µl for epididymal regions from PND40 and PND120; 0.5 ng/µL or 10 ng/ µL for epididymis from surgical castrated rats and EDL), under the cycling conditions of 2 min at 50°C, 3 min at 95°C, followed by 40 cycles of 15 s at 95°C and 1 min at 60°C. The quantification cycle (Cq; [28]) was determined automatically using the 7500 Applied Biosystems software (version 2.0.5). The average Cq value > 31 was set as a threshold for low expressed transcripts based on the literature. [29, 30]

Relative quantification of target genes was calculated using the $2^{-\Delta\Delta Cq}$ method. [31] The housekeeping gene *Rpl19* (Ribosomal protein L19) was used for internal standardization of qPCR results, since it is stably expressed during mesonephric duct morphogenesis and postnatal development of the epididymis. [22] Normalized qPCR data were expressed relative to their corresponding experimental reference group, which varied depending on the experimental model used (details in Figure legends). The amplification efficiency values for each *Pdi* oligonucleotide pair (sense and antisense) were calculated from standard plots made from dilution series of control cDNA (adult rat caput epididymis). Efficiency of reactions for each *Pdi* oligonucleotide pair was calculated from the slope using the equation $E = [10^{(-1/slope)}] - 1$ (**Table S1**).

2.7 *In silico* analysis of PDI mRNA expression in human epididymis

The *PDI* gene expression patterns in the human epididymis were examined *in silico* by analyzing the microarray dataset deposited in the Gene Expression Omnibus (GEO; access number GSE141568). [3] Analysis was conducted across the distinct epididymal segments (1-3, representing efferent ducts; segments 4-6, 7 and 8 associated with caput, corpus, and cauda, respectively). This evaluation was carried out using Log2 robust multiarray analysis (RMA). [32] To ensure robust statistical findings, the adjusted p-value approach (Benjamini and Hochberg method), which effectively limits false discovery rate (FDR), was used to identify *PDI* genes that exhibited statistically significant expression trends across the epididymis. [3] Differentially expressed genes (DGEs) were identified using criteria that encompassed fold change (FC) calculations and adjusted p-values. Only values exceeding the qualifying threshold ≥ 2.0 (in Log2FC) and adjusted p-values < 0.05 were selected as DEG in the screening process. [3] Expression values were plotted as a heatmap that showcase the average expression values across replicates from three subjects (37, 50 and 52 years of age; [3]). The spectrum of the heatmap was set as shades of pink and blue corresponding to low and high intensity values, respectively, varying from 3.98 (pink) to 16.29 (blue). The graphical heatmap, values were represented from lowest to highest relative to epididymal segment 1, thereby facilitating a coherent understanding of the expression dynamics across the various epididymal segments. The expression values for *SPAG1*, *DEFB128*, *DEFB125*, and *ACTG2* genes were used as signature genes due to their distinct and enriched expression profiles in the efferent ductules, caput, corpus, and cauda epididymis, respectively, as previously reported. [3]

2.9 Statistical analysis

Data were analyzed using Prism 8.0 (GraphPad Software, San Diego, CA, USA). Normality of all statistical determinations was analyzed with the Shapiro-Wilk test. F test or Bartlett's test were used to assess the homogeneity of variances for two and more groups, respectively. For parametric data, Student's t-test was applied to experiments with two groups, and analysis of variance (One-way ANOVA) followed by the Bonferroni test for multiple comparisons was applied to experiments with three or more groups. Differences were considered statistically significant at $p < 0.05$. Results are presented as mean ± standard error of the mean (SEM).

3 RESULTS

3.1 Differential expression of *Pdi* mRNAs in reproductive and non-reproductive tissues from adult rats

We tested 20 of the 21 *Pdi* transcripts in the caput epididymis from adult rats through semi-quantitative RT-PCR. All 20 amplicons were produced within their expected size and nucleotide sequence (data not shown). We next examined the expression profile of ten *Pdi* genes (*P4hb*, *Pdia2, Pdia3*, *Pdia5*, *Pdia6*, *Erp29*, *Erp44, Casq1*, *Casq2*, and *Pdilt*) in various reproductive and non-reproductive adult rat tissues by semi-quantitative RT-PCR (**Fig.1**). Of these genes, *P4hb***,** *Pdia3*, *Pdia5*, *Pdia6*, *Erp44, Erp29*, and *Casq1* mRNA levels were ubiquitously detected in all tissues examined, including epididymal regions (caput, corpus and cauda). *Casq2* mRNA was present in greater abundance in the vas deferens, prostate, and heart. *Pdilt* transcripts were detected in the testis (which was used as positive control; [33]) and caput epididymis. Conversely, *Pdia2* mRNA was detected more abundantly in the heart (which served as another a positive control; [18]), yet displayed minimal to low levels in the epididymis and other examined tissues (**Fig.1**).

3.2. Differential expression of PDI genes in the human epididymis by *in silico* analysis

Expression of all PDI genes was detected in all human epididymal segments (**Fig.2A**). We used segment 1-3 as the reference region (efferent ductules; ED) for clustering the results in terms of signal intensity (pink to blue colors; lowest to highest expression). Our transcriptome analysis data for *SPAG1*, *DEFB128*, *DEFB125*, and *ACTG2* along the human epididymal segments confirmed the previous results from Légaré and Sullivan for these same genes [3] and served as a consistent point of reference for our *in silico* analysis data (**Fig.2B**).

We observed that all PDIs are equally expressed or even more expressed along epididymal caput, corpus and cauda segments than along efferent ductules segments, except for *AGR3* (**Fig.2A**). Among the profiled PDIs in adult rats, *P4HB, PDIA3,* and *PDIA6*, for example, were more strongly expressed than *PDIA5*, *ERP29*, *PDILT, CASQ2, CASQ1* and *PDIA2* in human epididymal segments (4-8). As in the rat, the analysis revealed *PDIA2* with low expression levels in this tissue.

When analyzing the differentially expressed PDI genes ($log2FC \geq 2$, adj p-value < 0.05) in comparison to pairs of human epididymal regions, we found higher expression of *DNAJC10* (PDIA19) and *AGR2* in caput and

corpus than in ED, of *PDIA6* in corpus than in ED, of *ERP27* in corpus and cauda than in ED and caput, and of *CASQ2* in cauda than in caput. *AGR3* was the only PDI gene more expressed in ED than in caput, corpus or cauda. No DEGs were observed between corpus and cauda (**Fig.2C**).

3.3 Transcriptional profiling of *Pdi* genes in the rat prenatal and postnatal epididymis

We then focused qPCR analysis on a subset of six *Pdi* genes (*P4hb*, *Pdia3*, *Pdia5*, *Pdia6*, *Pdilt* and *Erp29*) to examine their developmental transcriptional profile in the rat epididymis. As shown in **Fig.3**, mRNA levels of *P4hb*, *Pdia3*, *Pdia5,* and *Pdia6* were readily detectable in the mesonephric ducts at both GD17.5 (uncoiled duct) and GD20.5 (coiled duct), a period when its morphogenesis is triggered by a significant increase in fetal plasma concentrations of testosterone. [22] The relative expression of these *Pdi* transcripts exhibited a two- to threefold increase between GD17.5 and GD20.5, paralleling to the expected decrease in relative levels of the androgen-dependent *Spag11c* mRNA that occurs in this time window and served as a positive control (**Fig.3**; [22]). In contrast, when comparing GD17.5 and GD20.5 mesonephric ducts, the detected *Erp29* transcript level remained stable (**Fig.3**), whereas *Pdilt* mRNA was expressed at very low abundance in both groups (**Table S2**).

Next, we tested the expression profile of these *Pdi* genes in the rat epididymis during postnatal development. As shown in **Fig.4**, only *Pdia5* and *Pdia6,* showed significant trends in their transcript levels during postnatal development PND1 to PND20 (whole epididymal samples), when the epididymis has not yet completed its development and maturation [1]; compared to their expression levels in our reference of PND1, *Pdia5* and *Pdia6* displayed higher abundance in the caput region of PND40 (immature rats) and PND120 (adult rats) than in the corpus and cauda epididymis on the same days (**Fig.4**). Transcript abundance of *P4hb*, *Pdia3*, and *Erp29* was not affected significantly by age when postnatal development between PND1 and PND20 or when the individual epididymal regions at PND40 and PND120 were compared. Similar to prenatal epididymis, the relative expression of *Pdilt* mRNA continued to be low in the epididymis from neonatal, prepubertal and adult rats (**Fig.4**; **Tables S2 and S3**). In these studies, the expression profile of *Grlx3* mRNA remained relatively constant among samples and therefore served as a control for the studies (**Fig.4**).

3.4 Influence of androgens and testicular factors on *Pdi* gene expression in the epididymis of adult rats

To investigate whether the expression of *Pdi* transcripts was modulated by androgens, we performed RT-qPCR using total RNA from caput epididymis of rats subjected to bilateral surgical castration for 7 and 15 days (**Fig.5**; **Table S4**). The relative expression of *P4hb*, *Pdia3*, *Pdia5*, *Pdia6*, *Pdilt,* and *Erp29* mRNA was significantly downregulated in samples from 7- and 15-days castrated rats, compared with the sham-operated control group. In 7 days castrated rats, supplementation with testosterone propionate for additional 6 consecutive days (7dT group) did not restore (*Pdilt*), partially restored *(P4hb*) or restored (*Pdia3*, *Pdia5*, *Pdia6,* and *Erp29*) mRNA levels of these *Pdi* genes in the caput epididymis to their control levels when compared with castration alone, indicating positive androgen modulation. The higher levels of *Ar* mRNA induced by surgical castration that returned to normal by testosterone treatment served as an internal control for these tests (**Fig.5**; **Table S4**).

To test whether testicular factors influence *Pdi* gene expression, we performed RT-qPCR on epididymal samples from rats subjected to either a sham procedure (CTL) or EDL (**Fig.6**; **Table S5**). The relative expression of *Pdia3*, *Pdia5*, *Pdia6*, *Pdilt,* and *Erp29* mRNA in the initial segment or caput epididymis was comparable when tissues from control and EDL rats were compared. As for *P4hb*, its mRNA level decreased only in caput epididymis following EDL, suggesting a potential role of testicular factors in the transcriptional regulation of this particular *Pdi* gene (**Fig.6**; **Table S5**).

4 DISCUSSION

Epididymal physiology supports sequential and continuous changes to the sperm on their way through the tissue, enabling them to reach, recognize, fuse with and fertilize the female gamete. During this maturation process, the protein composition of the epididymal fluid depends on both sequential secretion and specific reabsorption of proteins by the epithelial cells lining the epididymal tubule. To function properly, most of these epididymal proteins require controlled oxidative protein folding. Understanding the control system that governs the quality of secretory and membrane proteins in the epididymis not only enhances our understanding of epididymal biology but also paves the way to unveil new markers of sperm quality and fertility.-Here, we elucidate three key features

of the transcriptional landscape of *Pdi* genes in the epididymis that highlight the potential of the proteins they encode to be important for epididymal biology.

First, through a combination of our preclinical analysis (semi-quantitative and quantitative PCR) and *in silico* study of a human epididymal transcriptome [3], we uncovered a considerable number of *Pdi* genes expressed at varying levels in both adult rat and human epididymis. The co-expression of epididymal PDIs highlights the potential range of quality control which may involve these multifunctional proteins.

Second, we discovered constitutive expression of *P4hb*, *Pdia3*, *Pdia5*, *Pdia6*, *Erp29*, *Erp44, Casq1* and *Casq2* transcripts in the epididymis and other selected tissues tested from adult rats. In addition, *Pdilt* displayed predominant expression in the testis as expected [33, 34], with lower abundance also in the proximal epididymis. *Pdia2* transcript, while highly expressed in the heart, was present only at low levels in the adult rat epididymis, if detected at all - consistent with the findings of Fu *et al*. [18] Apart from the relative absence/low abundance of *Pdia2* mRNA in both adult rat and human epididymis, no clear signature of an epididymis-specific *Pdi* gene expression hierarchy became evident when compared to other peripheral tissues. In both, rat and human epididymis, *P4HB*, *PDIA3*, *PDIA6* and *ERp44* transcripts were enriched, while *CASQ1*, *CASQ2*, *PDIA2* and *PDILT* were relatively less abundant in both species. In contrast, *PDIA5* and *ERp29* showed lower relative expression in human epididymal tissue when compared to rats.

Third, by narrowing the focus to six *Pdi* genes, we uncovered relationships between tissue development and the impact of androgen plasma levels on the transcriptional profile of *Pdi* genes in the epididymis. All six of these genes, namely *P4hb*, *Pdia3*, *Pdia5, Pdia6, Pdilt and Erp29*, were continuously expressed in the rat prenatal and postnatal epididymis. Prenatally, the relative expression of these *Pdi* genes, with the exception of *Pdilt* and *Erp29* (which remained stable), increased between GD17.5 and GD20.5 in mesonephric ducts, the gestational time window for duct morphogenesis and a corresponding increase in circulating testosterone in male rat fetuses. [1, 5]

Postnatally, varying mRNA levels for *P4hb*, *Pdia3*, *Pdia5*, *Pdia6*, *Pdilt* and *Erp29* were detected from PND1 to PND120, with only the mRNA levels of *Pdia5* and *Pdia6* exhibiting an age-dependent increase during this period. In addition, the mRNAs of *Pdia3*, *Pdia5*, *Pdia6* and *Erp29* behaved as androgen-dependent transcripts; their reduced levels with surgical castration were reversed by exogenous testosterone. Although the mRNA levels

of *Pdilt* and *P4hb* were also significantly reduced after surgical castration, the castration-related effects on *Pdilt* mRNA levels were unaffected by testosterone treatment, and *P4hb* mRNA levels were only partially restored to control levels. In fact, *P4hb* mRNA levels were unique in responding to removal of testicular factors by EDL as well as removal of androgens by castration. Further studies are needed to illuminate whether these influences on *Pdilt* expression are sequential, summational, or synergistic.

The Nuclear Receptor Signaling Atlas (NURSA) platform, which we employed to predict relationships between androgens/androgen receptor signaling and *Pdi* gene expression [35], supports both up- [36] and down-regulation [37] of *P4hb* (and other *Pdi* genes), depending upon the androgen-responsive model chosen (**Table S6**). In the literature, *P4hb* and *Pdia3* transcripts were reported to increase in the epididymis of an adult boar GnRH-immunocastration model, suggesting higher levels of these PDIs during hypogonadism. [38] Additional support for the importance of the androgen-dependence of *P4hb* transcription in male reproductive tract tissues has been shown in prostate of adult mice. [39] Thus, these data suggest that various PDI mRNAs are differentially modulated and/or involved in discrete androgen-dependent events in the developing and the mature adult epididymis.

How do PDI-family proteins affect epididymal cell function? Further research is needed to expand on the roles of these PDIs, particularly for *Pdia3*, *Pdia5*, *Pdia6* and *Erp29,* which strongly display androgen dependence in the epididymal tissue in the present study. The literature is still scarce on both qualitative and quantitative data for the impact PDIs exert within the epididymis, but studies highlighting PDI roles in various animal models hint strongly for their participation in key reproductive events and processes. Examples of these PDIs are P4HB, PDIA3, PDIA6, ERp29 and PDILT, all PDIs with both testicular and epididymal origin and that have also been found to persist as sperm-associated proteins in the epididymal lumen; their thiol-disulfide activity affects sperm capacitation and fertilizing ability. [6,40-46] Further studies at the protein level can simultaneously confirm sites of synthesis and shed light on their roles within epididymal cells, especially in association with the ER. In this manner, we can better dissect their involvement in epididymal biology and sperm maturation.

Turning our focus to development, data in the literature point to an age-related decline in P4HB levels in testicular seminiferous tubules from prepubertal to adult swamp buffalo [47], while increasing in the cauda epididymal fluid from puberty to adulthood in stallions. [48] Our data in the prenatal and postnatal developing rat

mesonephric duct and epididymis are indicative of members of the PDI family as proteins exhibiting potential participation in these events, maybe involving additional mechanisms besides their primary role in protein quality control. Prenatally PDIs have been shown to influence embryonic development [49,50], epithelial-mesenchymal transition (ERp29 [51], AGR2 [52]), cell migration (PDI/P4HB [53, 54]), and other events related to tissue cell development and remodeling. [8,34,55,56] Future research to confirm the synthesis and the site of action of multiple PDIs, especially during the mesonephric/epididymal duct morphogenesis, should expand our knowledge of PDI protein family function.

As we have mentioned earlier, the PDI-related modulation of the intracellular concentration, storage and action of steroid hormones and their implications on epididymal function has been underappreciated. In fact, by functioning as binding proteins for estrogens (17β-estradiol), P4HB and PDIA2 affect estrogen action and the estrogen receptor ratio (ESR2/ESR1) in peripheral tissues such as pancreas. [17,57,58] PDIA2, via its hydrophobic pocket between the b and b'domains, may serve as an intracellular estrogen storage protein in human pancreas. [58] This b-type domain of PDI, responsible for both peptide and steroid hormone binding, is shared among family members involved in male fertility, such as PDIA3 and PDILT. It has also been reported that androgens, such as 19-nortestosterone, can enhance P4HB reductase activity, an effect that is reversed by increasing concentrations of estrogens. [59]

In humans, PDIA3 has been associated with male fertility [60,61], and autoantibodies against this protein in seminal plasma has been linked to chronic autoimmune orchitis and infertility in rats. [62,63] Also in humans, PDIA1 has been identified as a potential inhibitory target for hormone-induced suppression of spermatogenesis [64], while testicular PDILT autoantibodies has been associated with autoimmune polyendocrine syndrome type 1 in male patients, in which infertility is common.[65] Knockout mice lacking quality control genes such as *Pdilt* and *Clgn* (calmegin) are infertile due to a defect in production of ADAM3 sperm-egg binding protein in the testes. [67,68] In boars, elevated PDIA4 levels were correlated with good freezing ability of stored spermatozoa. [66] Despite these findings, questions remain on epididymal ER mechanisms and their contribution to male fertility.

The critical role of PDIs in male gamete biology and fertility, particularly in the context of the epididymis, warrants further investigation. Overall, our results provide a molecular foundation for understanding the roles of

multiple PDIs in epididymal development, maintenance, and normal function, particularly processes responsive to androgen regulation.

ACKNOWLEDGMENTS

The authors thank Gui Mi Ko, Jacilene Barbosa, Priscila Sartorio, and Joel M. Gabrilli for technical assistance, and Dr. Erick JR Silva (UNESP, Botucatu-SP, Brazil) for his support with data analysis. We also thank Dr. Christine Légaré and Dr. Robert Sullivan from Quebec-Université Laval Research Center, Québec, QC, Canada for sharing the human epididymal transcriptome data.

CONFLICT OF INTEREST STATEMENT

The authors declare no conflict of interest.

FUNDING INFORMATION

This study was financially supported by the São Paulo Research Foundation FAPESP (#2017/05261-8 to SGF; Sprint-FAPESP #2015/50011-4 to MCWA and AB), the Conselho Nacional de Desenvolvimento Científico e Tecnológico (CNPq, research grant award #311179/2016-9 to MCWA), and Coordenação de Aperfeiçoamento de Pessoal de Nível Superior (CAPES), Brazil.

DATA AVAILABILITY STATEMENT

The data that support the findings of this study are available from the corresponding author upon reasonable request.

AUTHOR CONTRIBUTIONS

SGF, AMB, and MCWA conceived the project. SGF and LGAF generated the data. SGF, LGAF, and MCWA performed the data analysis. SGF, LGAF, AMB and MCWA wrote the manuscript. All authors read and approved the final manuscript.

REFERENCES

1 Robaire B, Hinton BT. The Epididymis. Knobil Neills Physiol. Reprod., vol. 1: Elsevier; 2015: 691–771.

2 Sullivan R, Légaré C, Lamontagne-Proulx J, et al. Revisiting structure/functions of the human epididymis. Andrology. 2019;7:748–757. Doi: 10.1111/andr.12633.

3 Légaré C, Sullivan R. Differential gene expression profiles of human efferent ducts and proximal epididymis. Andrology. 2020;8:625–636. Doi: 10.1111/andr.12745.

4 Rodriguez-Martinez H, Roca J, Alvarez-Rodriguez M, et al. How does the boar epididymis regulate the emission of fertile spermatozoa? Anim Reprod Sci. 2022;246:106829. Doi: 10.1016/j.anireprosci.2021.106829.

5 Hinton BT, Avellar MCW. Wolffian Duct Development. Encycl. Reprod.: Elsevier; 2018: 256–262.

6 Björkgren I, Sipilä P. The impact of epididymal proteins on sperm function. Reproduction. 2019;158:R155–R167. Doi: 10.1530/REP-18-0589.

7 Benham AM. The Protein Disulfide Isomerase Family: Key Players in Health and Disease. Antioxid Redox Signal. 2012;16:781–789. Doi: 10.1089/ars.2011.4439.

8 Grek C, Townsend DM. Protein Disulfide Isomerase Superfamily in Disease and the Regulation of Apoptosis. Endoplasmic Reticulum Stress Dis. 2014;1. Doi: 10.2478/ersc-2013-0001.

9 Vendrely E, Dadoune JP. Quantitative ultrastructural analysis of the principal cells in the human epididymis. Reprod Nutr Dév. 1988;28:1225–1235. Doi: 10.1051/rnd:19880803.

10 Hatahet F, Ruddock LW. Protein Disulfide Isomerase: A Critical Evaluation of Its Function in Disulfide Bond Formation. Antioxid Redox Signal. 2009;11:2807–2850. Doi: 10.1089/ars.2009.2466.

11 Galligan JJ, Petersen DR. The human protein disulfide isomerase gene family. Hum Genomics. 2012;6:6. Doi: 10.1186/1479-7364-6-6.

12 Krossa S, Scheidig AJ, Grötzinger J, et al. Redundancy of protein disulfide isomerases in the catalysis of the inactivating disulfide switch in A Disintegrin and Metalloprotease 17. Sci Rep. 2018;8:1103. Doi: 10.1038/s41598-018-19429-4.

13 Soares Moretti AI, Martins Laurindo FR. Protein disulfide isomerases: Redox connections in and out of the endoplasmic reticulum. Arch Biochem Biophys. 2017;617:106–119. Doi: 10.1016/j.abb.2016.11.007.

14 Linden LDS, Bustamante-Filho IC, Souza APB, et al. Structural modelling of the equine protein disulphide isomerase A1 and its quantification in the epididymis and seminal plasma. Andrologia. 2020;52. Doi: 10.1111/and.13530.

15 Robinson PJ, Kanemura S, Cao X, et al. Protein secondary structure determines the temporal relationship between folding and disulfide formation. J Biol Chem. 2020;295:2438–2448. Doi: 10.1074/jbc.RA119.011983.

16 Miyake Y, Hashimoto S, Sasaki Y, et al. Endoplasmic Reticulum Protein (ERp) 29 Binds As Strongly As Protein Disulfide Isomerase (PDI) to Bisphenol A. Chem Res Toxicol. 2014;27:501–506. Doi: 10.1021/tx400357q.

17 Primm TP, Gilbert HF. Hormone Binding by Protein Disulfide Isomerase, a High Capacity Hormone Reservoir of the Endoplasmic Reticulum. J Biol Chem. 2001;276:281–286. Doi: 10.1074/jbc.M007670200.

18 Fu X-M, Dai X, Ding J, et al. Pancreas-specific protein disulfide isomerase has a cell type-specific expression in various mouse tissues and is absent in human pancreatic adenocarcinoma cells: implications for its functions. J Mol Histol. 2009;40:189–199. Doi: 10.1007/s10735-009-9230-5.

19 Karamzadeh R, Karimi-Jafari MH, Saboury AA, et al. Red/ox states of human protein disulfide isomerase regulate binding affinity of 17 beta-estradiol. Arch Biochem Biophys. 2017;619:35–44. Doi: 10.1016/j.abb.2017.02.010.

20 Diaz Cruz MA, Karlsson S, Szekeres F, et al. Differential expression of protein disulfide-isomerase A3 isoforms, PDIA3 and PDIA3N, in human prostate cancer cell lines representing different stages of prostate cancer. Mol Biol Rep. 2021;48:2429–2436. Doi: 10.1007/s11033-021-06277-1.

21 Karlsson S, Diaz Cruz MA, Faresjö M, et al. Inhibition of CYP27B1 and CYP24 Increases the Anti-proliferative Effects of 25-Hydroxyvitamin D 3 in LNCaP Cells. Anticancer Res. 2021;41:4733–4740. Doi: 10.21873/anticanres.15288.

22 Ribeiro CM, Queiróz DBC, Patrão MTCC, et al. Dynamic changes in the spatio-temporal expression of the β-defensin SPAG11C in the developing rat epididymis and its regulation by androgens. Mol Cell Endocrinol. 2015;404:141–150. Doi: 10.1016/j.mce.2015.01.013.

23 Ribeiro CM, Ferreira LGA, Thimoteo DS, et al. Novel androgen-induced activity of an antimicrobial β-defensin: Regulation of Wolffian duct morphogenesis. Mol Cell Endocrinol. 2017;442:142–152. Doi: 10.1016/j.mce.2016.12.016.

24 Queiróz DBC, Mendes FR, Porto CS, et al. α1-Adrenoceptor Subtypes in Rat Epididymis and the Effects of Sexual Maturation1. Biol Reprod. 2002;66:508–515. Doi: 10.1095/biolreprod66.2.508.

25 Mendes FR, Hamamura M, Queiróz DBC, et al. Effects of androgen manipulation on α1-adrenoceptor subtypes in the rat seminal vesicle. Life Sci. 2004;75:1449–1463. Doi: 10.1016/j.lfs.2004.03.011.

26 Nicander L, Osman DI, Pløen L, et al. Early effects of efferent ductule ligation on the proximal segment of the rat epididymis. Int J Androl. 1983;6:91–102. Doi: 10.1111/j.1365-2605.1983.tb00326.x.

27 Siu ER, Yasuhara F, Maróstica E, et al. Expression and localization of muscarinic acetylcholine receptor subtypes in rat efferent ductules and epididymis. Cell Tissue Res. 2006;323:157-166. Doi: 10.1007/s00441-005-0054-7.

28 Bustin, S.A., Vendesompele, J., Pfallf, M.W. Standardization of qPCR and RT-qPCR. Genet Eng Biotech News GEN. n.d.;29.

29 Kuang J, Yan X, Genders AJ, et al. An overview of technical considerations when using quantitative real-time PCR analysis of gene expression in human exercise research. PLOS ONE. 2018;13:e0196438. Doi: 10.1371/journal.pone.0196438.

30 Waseem H, Jameel S, Ali J, et al. Contributions and Challenges of High Throughput qPCR for Determining Antimicrobial Resistance in the Environment: A Critical Review. Molecules. 2019;24:163. Doi: 10.3390/molecules24010163.

31 Livak KJ, Schmittgen TD. Analysis of Relative Gene Expression Data Using Real-Time Quantitative PCR and the 2−ΔΔCT Method. Methods. 2001;25:402–408. Doi: 10.1006/meth.2001.126232

32 Irizarry RA, Bolstad, B. M., Collin, F., et al. Summaries of Affymetrix GeneChip probe level data. Nucleic Acids Res. 2003;31:15e–115. Doi: 10.1093/nar/gng015.

33 Van Lith M, Hartigan N, Hatch J, et al. PDILT, a Divergent Testis-specific Protein Disulfide Isomerase with a Non-classical SXXC Motif That Engages in Disulfide-dependent Interactions in the Endoplasmic Reticulum. J Biol Chem. 2005;280:1376–1383. Doi: 10.1074/jbc.M408651200.

34 Van Lith M, Karala A-R, Bown D, et al. A Developmentally Regulated Chaperone Complex for the Endoplasmic Reticulum of Male Haploid Germ Cells. Mol Biol Cell. 2007;18:2795–2804. Doi: 10.1091/mbc.e07-02-0147.

35 Becnel LB, Darlington YF, Ochsner SA, et al. Nuclear Receptor Signaling Atlas: Opening Access to the Biology of Nuclear Receptor Signaling Pathways. PLOS ONE. 2015;10:e0135615. Doi: 10.1371/journal.pone.0135615.

36 Welsbie DS, Xu J, Chen Y, et al. Histone Deacetylases Are Required for Androgen Receptor Function in Hormone-Sensitive and Castrate-Resistant Prostate Cancer. Cancer Res. 2009;69:958–966. Doi: 10.1158/0008-5472.CAN-08-2216.

37 Snyder EM, Small CL, Li Y, et al. Regulation of Gene Expression by Estrogen and Testosterone in the Proximal Mouse Reproductive Tract1. Biol Reprod. 2009;81:707–716. Doi: 10.1095/biolreprod.109.079053.

38 Schorr-Lenz AM, Alves J, Henckes NAC, et al. GnRH immunization alters the expression and distribution of protein disulfide isomerases in the epididymis. Andrology. 2016;4:957–963. Doi: 10.1111/andr.12205.

498 39 Fujimoto N, Akimoto Y, Suzuki T, et al. Identification of prostatic-secreted proteins in mice by mass spectrometric
499 analysis and evaluation of lobe-specific and androgen-dependent mRNA expression. J Endocrinol. 2006;190:793–803.
500 Doi: 10.1677/joe.1.06733.
501 40 Ohtani H, Wakui H, Ishino T, et al. An isoform of protein disulfide isomerase is expressed in the developing acrosome of
502 spermatids during rat spermiogenesis and is transported into the nucleus of mature spermatids and epididymal
503 spermatozoa. Histochemistry. 1993;100:423–429. Doi: 10.1007/BF00267822.
504 41 Kameshwari DB, Bhande S, Sundaram CS, et al. Glucose-regulated protein precursor (GRP78) and tumor rejection antigen
505 (GP96) are unique to hamster caput epididymal spermatozoa. Asian J Androl. 2010;12:344–355. Doi:
506 10.1038/aja.2010.19.
507 42 Ellerman DA, Myles DG, Primakoff P. A Role for Sperm Surface Protein Disulfide Isomerase Activity in Gamete Fusion:
508 Evidence for the Participation of ERp57. Dev Cell. 2006;10:831–837. Doi: 10.1016/j.devcel.2006.03.011.
509 43 Zhang J, Wu J, Huo R, et al. ERp57 is a potential biomarker for human fertilization capability. Mol Hum Reprod.
510 2007;13:633–639. Doi: 10.1093/molehr/gam049.
511 44 Akama K, Horikoshi T, Sugiyama A, et al. Protein disulfide isomerase-P5, down-regulated in the final stage of boar
512 epididymal sperm maturation, catalyzes disulfide formation to inhibit protein function in oxidative refolding of reduced
513 denatured lysozyme. Biochim Biophys Acta BBA - Proteins Proteomics. 2010;1804:1272–1284. Doi:
514 10.1016/j.bbapap.2010.02.004.
515 45 Eletto D, Eletto D, Boyle S, et al. PDIA6 regulates insulin secretion by selectively inhibiting the RIDD activity of IRE1.
516 FASEB J. 2016;30:653–665. Doi: 10.1096/fj.15-275883.
517 46 Ying X, Liu Y, Guo Q, Qu F, et al. Endoplasmic reticulum protein 29 (ERp29), a protein related to sperm maturation is
518 involved in sperm-oocyte fusion in mouse. Reprod Biol Endocrinol. 2010;8:10. Doi: 10.1186/1477-7827-8-10.
519 47 Zhang P, Huang Y, Fu Q, et al. Comparative proteomic analysis of different developmental stages of swamp buffalo
520 testicular seminiferous tubules. Reprod Domest Anim. 2017;52:1120–1128. Doi: 10.1111/rda.13044.
521 48 Wilson R, Norris EL, Brachvogel B, et al. Changes in the Chondrocyte and Extracellular Matrix Proteome during Post-
522 natal Mouse Cartilage Development. Mol Cell Proteomics. 2012;11:M111.014159. Doi: 10.1074/mcp.M111.014159.
523 49 Hoshijima K, Metherall JE, Grunwald DJ. A protein disulfide isomerase expressed in the embryonic midline is required
524 for left/right asymmetries. Genes Dev. 2002;16:2518–2529. Doi: 10.1101/gad.1001302.

50 Afelik S, Chen Y, Pieler T. Pancreatic protein disulfide isomerase (XPDIp) is an early marker for the exocrine lineage of the developing pancreas in Xenopus laevis embryos. Gene Expr Patterns. 2004;4:71–76. Doi: 10.1016/S1567-133X(03)00150-9.

51 Zhang D, Richardson DR. Endoplasmic reticulum protein 29 (ERp29): An emerging role in cancer. Int J Biochem Cell Biol. 2011;43:33–36. Doi: 10.1016/j.biocel.2010.09.019.

52 Sommerova L, Ondrouskova E, Vojtesek B, et al. Suppression of AGR2 in a TGF-β-induced Smad regulatory pathway mediates epithelial-mesenchymal transition. BMC Cancer. 2017;17:546. Doi: 10.1186/s12885-017-3537-5.

53 Bi S, Hong PW, Lee B, et al. Galectin-9 binding to cell surface protein disulfide isomerase regulates the redox environment to enhance T-cell migration and HIV entry. Proc Natl Acad Sci. 2011;108:10650–10655. Doi: 10.1073/pnas.1017954108.

54 Torpe N, Gopal S, Baltaci O, et al. A Protein Disulfide Isomerase Controls Neuronal Migration through Regulation of Wnt Secretion. Cell Rep. 2019;26:3183-3190.e5. Doi: 10.1016/j.celrep.2019.02.072.

55 Lee E, Lee DH. Emerging roles of protein disulfide isomerase in cancer. BMB Rep. 2017;50:401–410. Doi: 10.5483/BMBRep.2017.50.8.107.

56 Li M, Li H, Yang H, et al. Comparative proteomic analysis of round and elongated spermatids during spermiogenesis in mice. Biomed Chromatogr. 2020;34:e4799. Doi: 10.1002/bmc.4799.

57 Fu X, Wang P, Zhu BT. Protein disulfide isomerase is a multifunctional regulator of estrogenic status in target cells. J Steroid Biochem Mol Biol. 2008;112:127–137. Doi: 10.1016/j.jsbmb.2008.09.005.

58 Fu X-M, Wang P, Zhu BT. Characterization of the Estradiol-Binding Site Structure of Human Pancreas-Specific Protein Disulfide Isomerase: Indispensable Role of the Hydrogen Bond between His278 and the Estradiol 3-Hydroxyl Group. Biochemistry. 2011;50:106–115. Doi: 10.1021/bi101451g.

59 Hassan MH, Alvarez E, Cahoreau C, et al. Potentiation of the reductase activity of protein disulphide isomerase (PDI) by 19-nortestosterone, bacitracin, fluoxetine, and ammonium sulphate. J Enzyme Inhib Med Chem. 2011;26:681–687. Doi: 10.3109/14756366.2010.546794.

60 Bohring C, Krause, E., Habermann, B., et al. Isolation and identification of sperm membrane antigens recognized by antisperm antibodies, and their possible role in immunological infertility disease. Mol Hum Reprod. 2001;7:113–118. Doi: 10.1093/molehr/7.2.113.

61 Bohring C, Krause W. Characterization of Spermatozoa Surface Antigens by Antisperm Antibodies and its Influence on Acrosomal Exocytosis. Am J Reprod Immunol. 2003;50:411–419. Doi: 10.1034/j.1600-0897.2003.00103.x.

62 Fijak M, Iosub R, Schneider E, et al. Identification of immunodominant autoantigens in rat autoimmune orchitis. J Pathol. 2005;207:127-138. Doi: 10.1002/path.1828.

63 Fijak M, Zeller T, Huys T, et al. Autoantibodies against protein disulfide isomerase ER-60 are a diagnostic marker for low-grade testicular inflammation. Hum Reprod. 2014;29:2382-2392. Doi: 10.1093/humrep/deu226.

64 Cui Y, Zhu H, Zhu Y, et al. Proteomic Analysis of Testis Biopsies in Men Treated with Injectable Testosterone Undecanoate Alone or in Combination with Oral Levonorgestrel as Potential Male Contraceptive. J Proteome Res. 2008;7:3984-3993. Doi: 10.1021/pr800259t.

65 Tong S, Yin C, Ge Y, et al. Albumin (ALB) and protein disulfide isomerase family A member 4 (PDIA4) are novel markers to predict sperm freezability of Erhualian boar. Cryobiology. 2022;109:37-43. Doi: 10.1016/j.cryobiol.2022.09.006.

66 Ikawa M, Wada I, Kominami K, et al. The putative chaperone calmegin is required for sperm fertility. Nature. 1997;387:607–611. Doi: 10.1038/42484.

67 Tokuhiro K, Ikawa M, Benham AM, et al. Protein disulfide isomerase homolog PDILT is required for quality control of sperm membrane protein ADAM3 and male fertility. Proc Natl Acad Sci. 2012;109:3850-3855. Doi: 10.1073/pnas.1117963109.

68 Landegren N, Sharon D, Freyhult E, et al. Proteome-wide survey of the autoimmune target repertoire in autoimmune polyendocrine syndrome type 1. Sci Rep. 2016;6:20104. Doi: 10.1038/srep20104.

FIGURE LEGENDS

FIGURE 1 *Pdi* mRNA profile by semi-quantitative PCR in adult rat reproductive and non-reproductive tissues. Assays were performed with cDNA from a representative tissue panel of one animal. *Gapdh* mRNA was used as an internal control (housekeeping gene). Negative control: absence of the cDNA template. Image is representative of an agarose gel stained with ethidium bromide; amplicons were observed at their expected size (**Table S1**). The vertical dotted line (black) separates the tissue sets (reproductive and non-reproductive tissues). Epididymal regions: caput (including initial segment), corpus and cauda regions. **Pdia2* mRNA was low/undetectable in most tissues tested; in this case, heart samples served as a positive control.

FIGURE 2 Clustering of *PDI* genes in human epididymis presented as a heat map. (A) Signal intensity acquired from the publicly available microarray is expressed as log2 RMA and represented in the heatmap by colors, from pink to blue colors (lowest to highest expression), to each individual epididymal segment (each row, from 1-8) and *Pdi* gene (each column). Clustering was based on signal intensity of the efferent ductules (segment 1). Data correspond to replicate-averaged from three subjects as reported. The PDI genes highlighted in blue color were tested in adult rat epididymis (see **Fig.1**). (B) Clustering of the *SPAG1*, *DEFB128*, *DEFB125* and *ACTG2* genes, transcriptomic signatures for the efferent ductules, caput, corpus and cauda, respectively. Results served as consistent point of reference for our *in silico* data, since they confirmed the previous results from Légare and Sullivan for these same genes[3], and therefore provided a common basis for further analysis. Results reflect the level of expression of these genes that represent region-specific signatures for each epididymal region tested. (C) Differentially expressed PDI genes based on GEO2R analysis between human epididymal segments, as indicated. Data is expressed as log2FC. ED: efferent ductules. DEG: differentially expressed genes.

FIGURE 3 *Pdi* mRNA relative expression during rat mesonephric duct/epididymal prenatal development. RT-qPCR was performed with cDNA samples from mesonephric ducts isolated from male rat fetuses of GD17.5 (uncoiled duct) and GD20.5 (coiled duct). (A and B) The data shown are qPCR relative quantification for each *Pdi* gene. (C) *Spag11c* gene was used as positive control due to its expected androgen-dependent decrease in this experimental model, as previously reported. [22,23] Transcript levels were normalized using *Rpl19* as the reference gene. Results are expressed relative to GD17.5 (reference group). Data are mean ± SEM ($N = 4$ ducts per group; assays were run in duplicates; see **Table S2** for Cq values). Statistical analysis: *Student t-test*; $*p < 0.05$.

FIGURE 4 Differential expression patterns of *Pdi* transcripts in the rat epididymis during postnatal development. RT-qPCR was performed using cDNA samples derived from whole epididymis (PND1-PND20) and in the epididymal regions (Ca: caput, including initial segment; Co: corpus; Cd: cauda) from prepubertal (PND40) and adult (PND120) rats. (A and B) The data shown are qPCR relative quantification for each *Pdi*

gene. (C) with *Glrx3* gene transcriptional profile used as a positive control. Transcript levels were normalized using *Rpl19* as the reference gene. Results are expressed relative to PND1 (reference group). Data are presented as mean ± SEM (N = 3-4 tissues from different rats, run in duplicates; see **Table S3** for Cq values). Different letters indicate significant differences when time points PND1-PND20 were compared; the number sign (#) denote statistical difference when compared to PND1; and asterisks (*) denote significant differences when epididymal regions (Ca, Co and Cd) from PND40 or PND120 were compared ($p < 0.05$; One-way ANOVA followed by Bonferroni test). No differences were observed in *Pdi* gene expression when each individual epididymal region from PND40 and PND120 rats was compared (*Student t-test*, $p > 0.05$). *Pdilt* exhibited a low expression level (Cq > 32), in contrast to other transcripts with Cq ranging from 23-28 (**Table S3**).

FIGURE 5 Effects of androgens on the *Pdi* transcriptional profile in adult rat epididymis. RT-qPCR was performed on cDNA samples from the caput (including initial segment) epididymis from rats (PND90) that were sham-operated (control; CTL), or surgically castrated for 7 (7d) or 15 days (15d), and castrated for 7 days and then treated with testosterone propionate, daily, for additional 6 consecutive days (7dT). (A and B) Shown are relative quantifications of *Pdi* mRNA levels, (C) with *Ar* gene expression used as a positive control. Transcript levels were normalized using *Rpl19* as the reference gene. Results are expressed relative to controls (reference group). Data are presented as mean ± SEM (N = 5-6 rats per group; assays conducted in duplicates; **Table S4** for Cq values). Statistical differences among groups are denoted by distinct letters (One-way ANOVA followed by Bonferroni, $p < 0.05$). *Pdilt* transcript profile refer to assays using a higher cDNA concentration (10 ng/µl of cDNA), which resulted in a 3-5 fold change in Cq values across experimental groups, although still consistently with Cq>31 (**Table S4**).

FIGURE 6 Effects of efferent ductules ligation on the *Pdi* transcriptional profile in adult rat epididymis. RT-qPCR was performed on cDNA samples from the initial segment (IS) and caput epididymis of adult rats (PND90) subjected to sham procedure (control, CTL; white bars) or efferent ductules ligation (EDL; gray bars) to study the modulation of *Pdi* transcripts by testicular factors. Shown are relative quantifications of *Pdi* mRNA

levels. Transcript levels were normalized using *Rpl19* as the reference gene. Results for each epididymal region are expressed relative to its respective control (reference group). Data are presented as mean ± SEM (N = 3-6 rats per group; assays conducted in duplicates; **Table S5** for Cq values). Statistical difference from the respective control is indicated by asterisks (*Student's t*-test; $p < 0.05$).

SUPPLEMENTAL MATERIALS

- Supplemental Figure S1,
- Supplemental Table S1
- Supplemental Table S2
- Supplemental Table S3
- Supplemental Table S4
- Supplemental Table S5
- Supplemental Table S6

Fig.1
Fernandes et al.

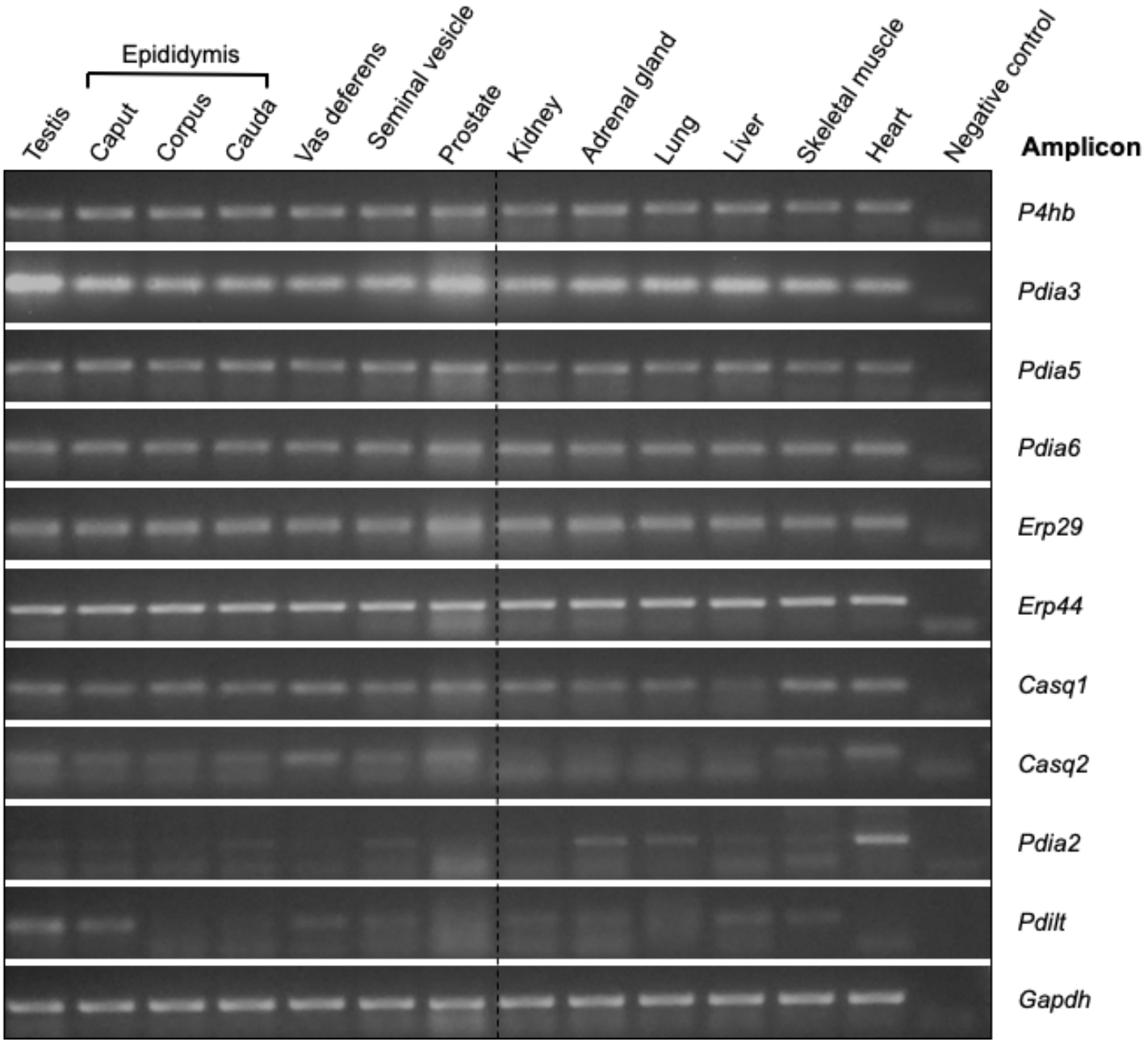

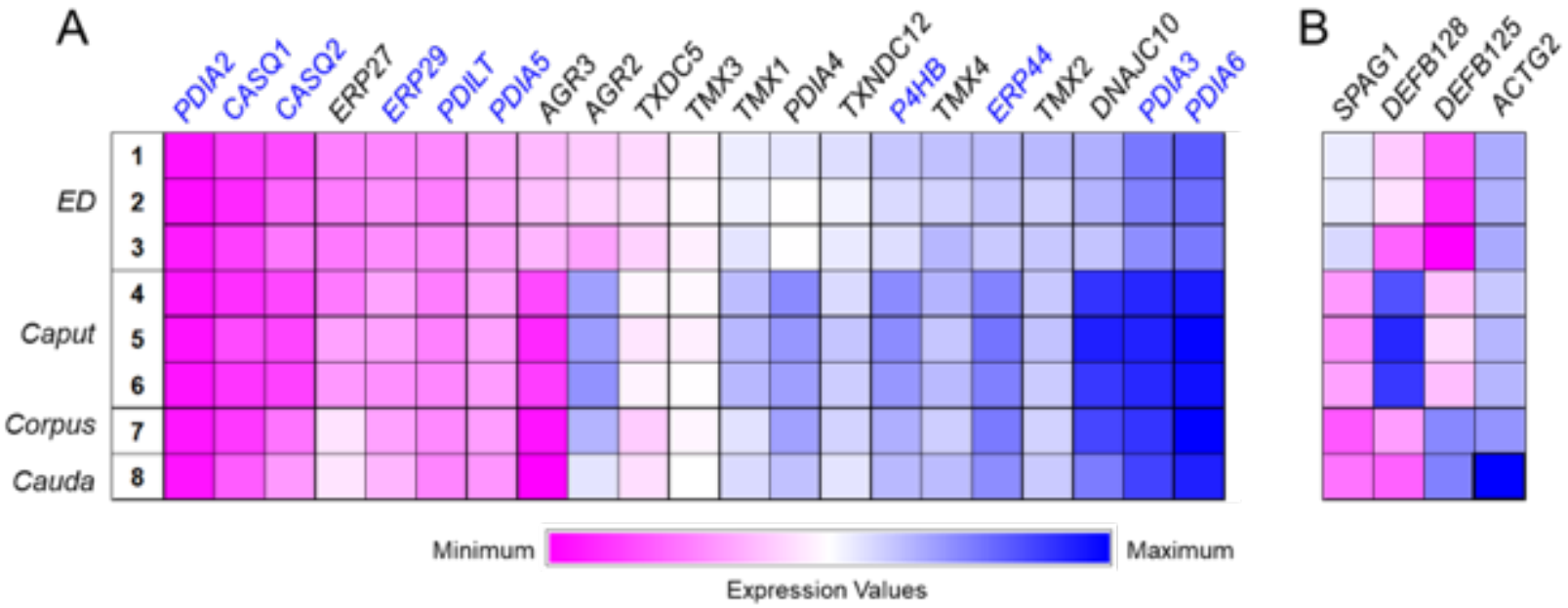

C

PDI mRNA	DEGs – Human Epididymal Segments				
	ED vs Caput	ED vs Corpus	ED vs Cauda	Caput vs Cauda	Caput vs Corpus
DNAJC10	-2.63	-2.17			
AGR2	-3.49	-2.99			
AGR3	3.27	4.27	4.73		
PDIA6		-2.04			
ERP27			-2.62	-2.11	-2.08
CASQ2				-2.16	

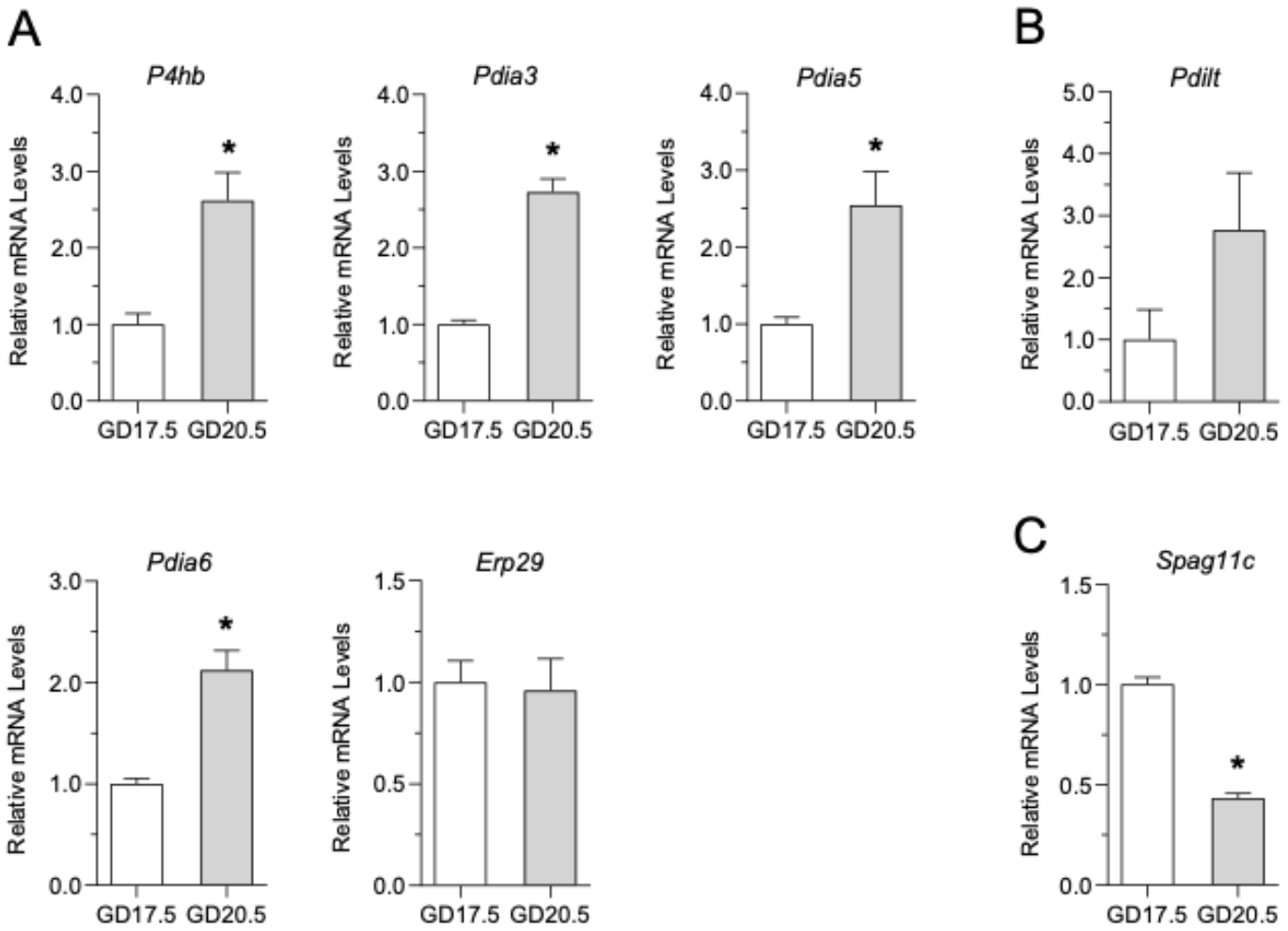
A
P4hb
Pdia3
Pdia5
Pdia6
Erp29
B
Pdilt
C
Spag11c
Relative mRNA Levels
GD17.5
GD20.5
*

Fig.4
Fernandes et al.

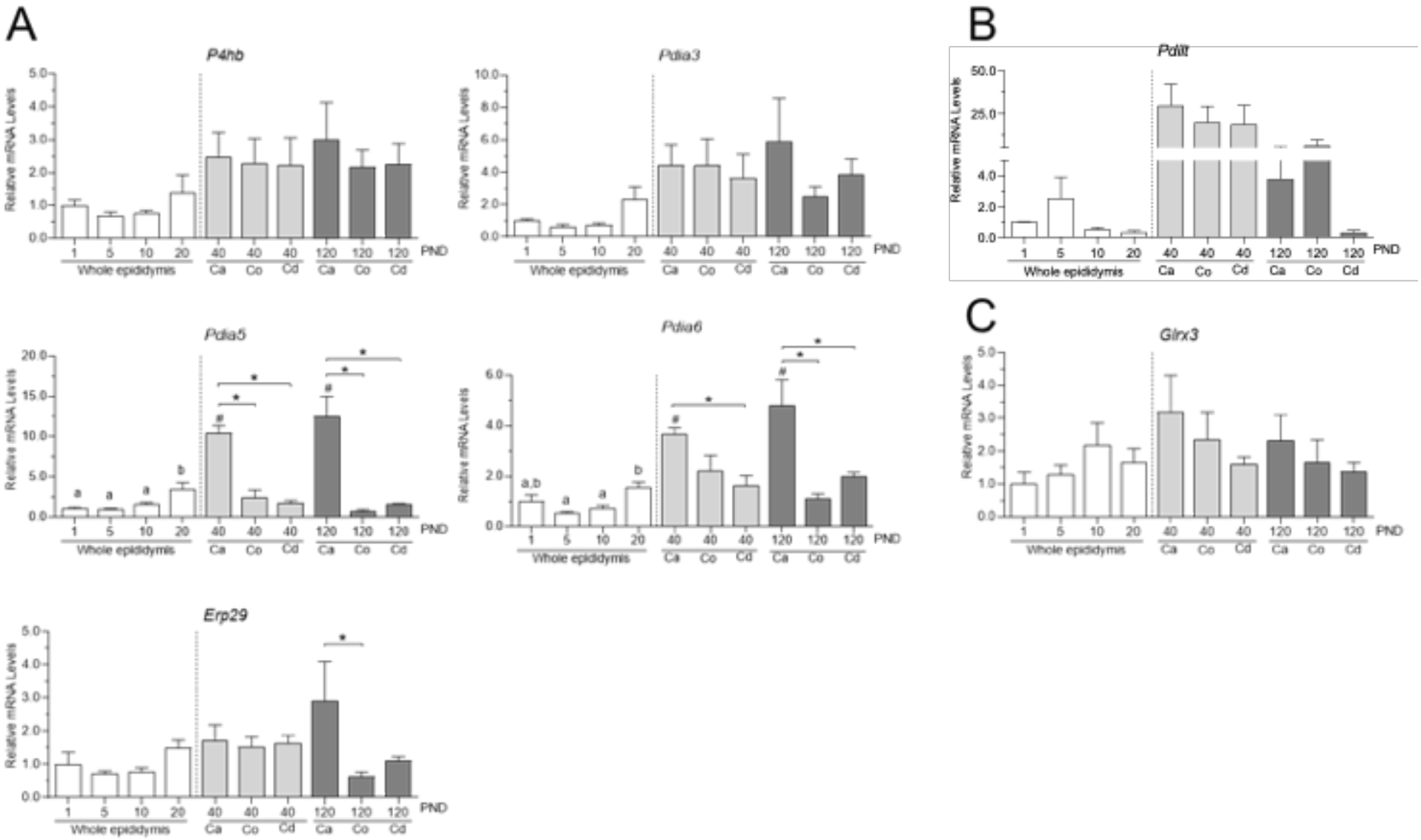

Fig.5
Fernandes et al.

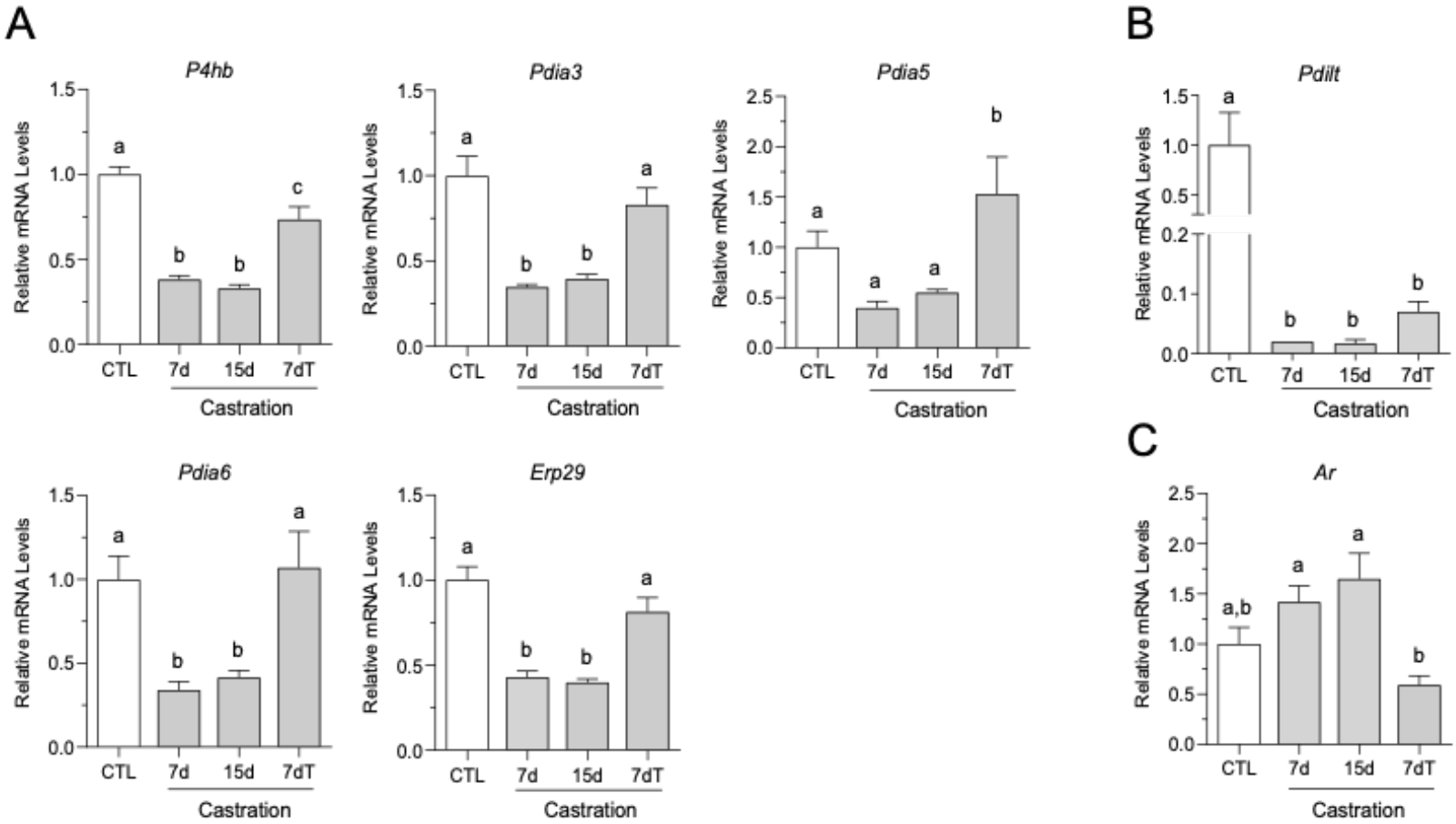

Fig.6
Fernandes et al.

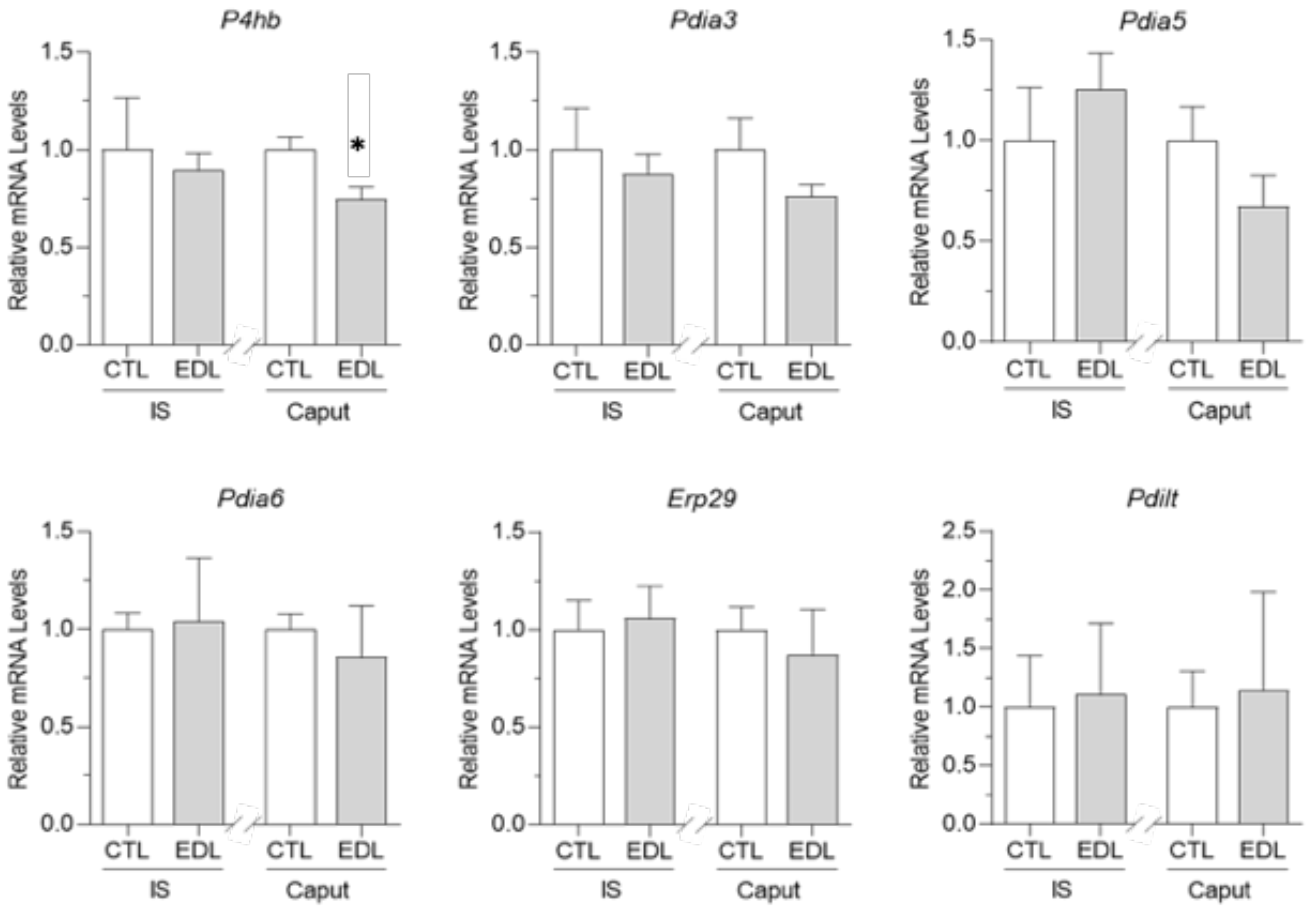

SUPPLEMENTAL FIGURE S1. Schematic representation of the domain composition of the 21 proteins in the *PDI* gene family. Sequence and domain composition can be verified at National Center for Biotechnology Information (NCBI) database. Subsets of PDIs are grouped in panels A, B and C (human and rat; protein synonyms are noted). All proteins contain a short N-terminal signal sequence (N). P4HB (also known as PDI and PDIA1) is the prototype PDI. The unifying theme between these proteins is the presence of at least one thioredoxin-like domain (TRX) whether this be catalytically active (**a** and **a'**; in blue) or inactive (**b** and **b'**; in pink). Catalytic motifs are denoted in active domains (classical sequence: CGHC). Violet: Asp/Glu rich Ca^{2+}-binding domains. Tangerine: transmembrane domains. Yellow: C-terminal ER retention signal sequences with amino acids composition denoted. The letter "X" is representing the linker regions. Figure was adapted and modified. [15]

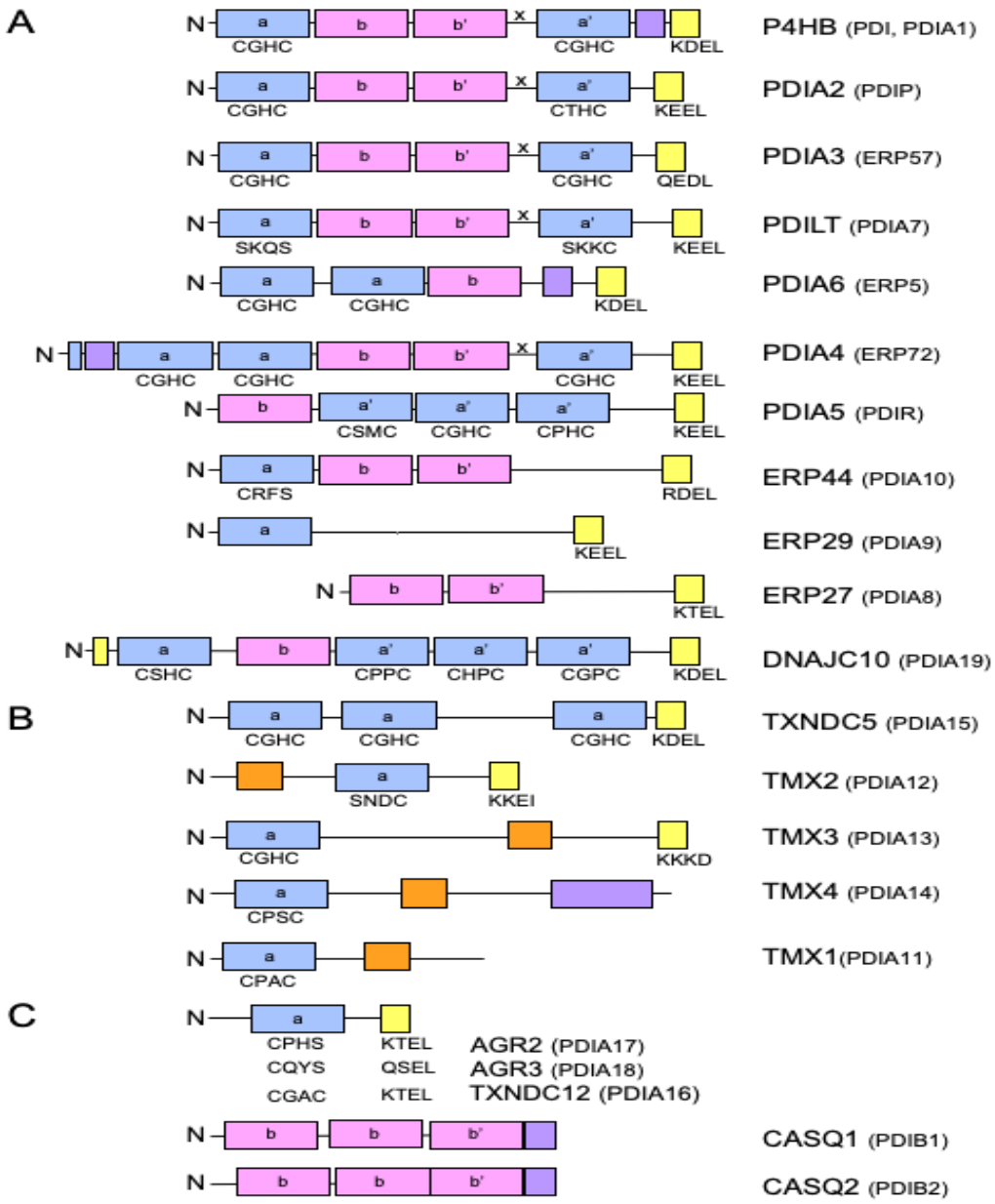

SUPPLEMENTAL TABLE S1. Oligonucleotide sequences used in RT-PCR. For each individual listed *Pdi* gene, the official nomenclature (https://www.genenames.org) and respective *National Center Biotechnology Information* (NCBI) accession number are provided. The oligonucleotide sequences (Forward, *F*; Reverse, *R*), expected amplicon size (in base pairs, bp) and correspondent amplification efficiency (*E%*) are shown (ND - Not Determined).

Transcripts	Accession Number		Sequence (5' - 3')	Amplicon (bp)	E (%)
P4hb (Pdia1) *Prolyl 4-Hydroxylase Subunit Beta*	NM_012998.2	F	CTGGTGGAGTTCTATGCCCC	140	103
		R	GCCAGGTCAGACTCTTCTGTG		
Pdia2 *Protein Disulfide Isomerase Family A Member 2*	NM_0011057752	F	CAGCCCTGATGGTGGAGTTT	220	91
		R	TCTTCTGGGTTTGTGCGGTT		
Pdia3 *Protein Disulfide Isomerase Family A Member 3*	NM_017319.1	F	GGCTTGCCCCTGAGTATGAA	75	99
		R	CAGTGCAGTCCACCTTTGCT		
Pdia5 *Protein Disulfide Isomerase Family A Member 5*	NM_001014125.1	F	GCGGCTCCGTTTATCACCTG	168	102
		R	CACCAGAGCTCTCAGCATCTCC		
Pdia6 *Protein Disulfide Isomerase Family A Member 6*	NM_001004442.1	F	TTCTCAGGGAACTGTCTTTCGG	129	99
		R	GGTCAATGTCGTCCTCCACA		
Pdilt *Protein Disulfide Isomerase Like, Testis Expressed*	NM_001013902.1	F	TCCACGTGATCCTTGACAGC	125	92
		R	ACCCGTGAGCTGTTGCTTTA		
Erp29 *Endoplasmic Reticulum Protein 29*	NM_053961.2	F	GGTGAAGTTCGACACCCAGT	120	96
		R	CCATAGTCTGAGATCCCCACCT		
Erp44 *Endoplasmic Reticulum Protein 44*	NM_001008317.1	F	CTGACTGGTGTCGTTTCAGC	220	ND
		R	GATCGCTGGCCCCTGTATTC		
Casq1 *Calsequestrin 1*	NM_001159594.1	F	TACCTTCGACAGCAAGGTGG	108	92
		R	CTGTTGGGCTTGTCTGGGAT		
Casq2 *Calsequestrin 2*	NM_017131.2	F	CGCCCAGAGGACATGTTTGA	93	ND
		R	CTCATAGCCATCTGGGTCACTC		
Ar *Androgen Receptor*	NM_012502	F	ACAACAACCAGCCTGATTCC	133	98
		R	ATCTGGTCATCCACATGCAA		
Glrx3 *Glutaredoxin 3*	NM_032614	F	AGCAAGCAGATGGTGGAAAT	243	90
		R	CAGCACTTTGAGCCTTTCCT		
β-def1 *Defensin Beta 1*	NM_031810.1	F	GACCCTGACTTCACCGACAT	222	93
		R	CCTGCAACAGTTGGGCTTAT		
Spag11c *Sperm Associated Antigen 11c*	NM_001037852	F	ACAGCCATGAAACGGAGACT	123	99
		R	AGTGACACCTGCTGAAAGAGC		
Gapdh *Glyceraldehyde-3-Phosphate Dehydrogenase*	NM_017008	F	AGACAGCCGCATCTTCTTCTTGT	207	97
		R	CTTGCCGTGGGTAGAGTCAT		
Rpl19 *Ribosomal Protein L19*	NM_031103	F	CAATGAAACCAACGAAATCG	71	99
		R	TCAGGCCATCTTTGATCAGCT		

SUPPLEMENTAL TABLE S2. Expression of *Pdi* transcripts in the developing mesonephric ducts of male rats. Quantification cycle (Cq) values from RT-qPCR studies performed with total RNA from mesonephric ducts of fetuses at gestational day (GD) 17.5 (uncoiled ducts) and GD20.5 (coiled ducts). Data are mean ± SEM of experiments performed with samples from the indicated number of male fetuses. *Rpl19* was used as the reference gene. The average Cq value > 31 was used as a cutoff for low-expression transcripts (see Methods).

Transcripts	Gestational Day Points (N=4)	
	GD17.5	GD20.5
P4hb	23.85 ± 0.31	22.69 ± 0.20
Pdia3	26.13 ± 0.19	24.89 ± 0.15
Pdia5	27.38 ± 0.22	26.30 ± 0.21
Pdia6	24.04 ± 0.09	23.18 ± 0.20
Erp29	26.64 ± 0.09	24.95 ± 0.17
Pdilt	35.96 ± 1.17	34.05 ± 0.54
Spag11c	23.96 ± 0.12	26.18 ± 0.74
Rpl19	21.07 ± 0.13	21.29 ± 0.20

SUPPLEMENTAL TABLE S3. Modulation of *Pdi* transcripts in the rat epididymis across postnatal development. Quantification cycle (Cq) values from RT-qPCR studies performed with total RNA from epididymis of rats at postnatal day (PND) 1, PND5, PND10, PND20 (whole epididymis), and in the epididymal regions (caput, including initial segment; corpus and cauda) from prepubertal (PND40) and adult (PND120) rats. Data are mean ± SEM of experiments performed with samples from 3-4 rats per group. *Rpl19* was used as the reference gene. The average Cq value > 31 was used as a cutoff for low-expression transcripts (see Methods).

Transcripts	Cq Values									
	Whole Epididymis				Epididymal Regions					
	PND1	PND5	PND10	PND20	PND40			PND120		
					Caput	Corpus	Cauda	Caput	Corpus	Cauda
P4hb	21.36 ± 0.37	21.79 ± 0.15	21.43 ± 0.40	21.54 ± 0.35	20.91 ± 0.73	21.07 ± 0.17	21.35 ± 0.54	20.43 ± 0.92	20.88 ± 0.34	20.43 ± 0.6
Pdia3	24.64 ± 0.31	25.28 ± 0.26	24.80 ± 0.53	24.08 ± 0.36	23.32 ± 0.66	23.47 ± 0.23	23.97 ± 0.54	22.82 ± 0.92	24.04 ± 0.23	23.45 ± 0.4
Pdia5	26.47 ± 0.40	26.37 ± 0.21	25.42 ± 0.41	25.07 ± 0.37	23.67 ± 0.01	26.08 ± 0.40	26.43 ± 0.49	22.65 ± 0.35	27.37 ± 0.24	26.34 ± 0.2
Pdia6	23.40 ± 0.52	24.06 ± 0.19	23.51 ± 0.50	23.05 ± 0.25	22.01 ± 0.15	22.92 ± 0.40	23.38 ± 0.53	20.96 ± 0.29	23.71 ± 0.35	22.86 ± 0.3
Erp29	25.98 ± 0.62	26.00 ± 0.29	25.82 ± 0.38	25.55 ± 0.34	25.67 ± 0.31	25.88 ± 0.41	25.80 ± .46	24.76 ± 0.46	27.02 ± 0.28	26.16 ± 0.3
Pdilt	34.28 ± 0.85	34.25 ± 0.82	34.41 ± 1.16	36.10 ± 0.99	32.42 ± 1.75	32.73 ± 0.93	33.54 ± 1.91	34.09 ± 0.84	34.09 ± 1.87	37.88 ± 0.5
Glrx3	25.19 ± 0.61	24.58 ± 0.51	23.76 ± 0.50	24.86 ± 0.25	24.15 ± 0.49	24.67 ± 0.54	24.59 ± 0.55	24.40 ± 0.58	25.08 ± 0.53	25.24 ± 0.2
Rpl19	19.30 ± 0.17	19.19 ± 0.18	19.01 ± 0.31	19.75 ± 0.17	20.01 ± 0.19	20.90 ± 0.36	20.11 ± 0.26	19.71 ± 0.15	19.93 ± 0.22	19.95 ± 0.2

SUPPLEMENTAL TABLE S4. Modulation of *Pdi* transcripts by androgens in adult rat epididymis. Quantification cycle (Cq) values from RT-qPCR studies performed with total RNA from caput (including initial segment) epididymis from rats (PND90) that were sham-operated (control; CTL) or surgically castrated for 7 (7d) or 15 days (15d). A separate group of rats was surgically castrated for 7 days and then treated with testosterone propionate (1 mg/kg of body mass, s.c.), daily, for 6 consecutive days, before euthanasia (7dT). Data are mean ± SEM of experiments performed with samples from 4-6 rats per group. *Rpl19* was used as the reference gene. The average Cq value > 31 was used as a cutoff for low-expression transcripts (see Methods).

Transcripts	**Experimental Groups**			
	Sham-Operated	Surgical Castration		
	CTL	7d	15d	7dT
P4hb	20.54 ± 0.19	21.99 ± 0.11	21.91 ± 0.18	21.32 ± 0.18
Pdia3	21.36 ± 0.11	22.90 ± 0.13	22.43 ± 0.14	21.95 ± 0.21
Pdia6	20.17 ± 0.05	24.36 ± 0.28	18.70 ± 0.17	19.47 ± 0.38
Erp29	23.34 ± 0.23	24.61 ± 0.18	24.41 ± 0.12	23.97 ± 0.17
Pdia5	23.93 ± 0.08	25.33 ± 0.28	24.47 ± 0.13	23.98 ± 0.56
Pdilt (10 ng)	27.84 ± 0.55	31.99 ± 0.81	34.43 ± 1.86	31.96 ± 0.40
Pdilt (5 ng)	32.43 ± 0.56	36.68 ± 0.45	37.28 ± 1.68	35.88 ± 0.84
Ar	23.78 ± 0.18	23.30 ± 0.24	22.86 ± 0.19	24.84 ± 0.28
Rpl19	20.22 ± 0.22	20.27 ± 0.12	19.97 ± 0.17	20.52 ± 0.19

SUPPLEMENTAL TABLE S5. Effects of efferent ductules ligation on the *Pdi* transcriptional profile in adult rat epididymis. Quantification cycle (Cq) values from RT-qPCR studies performed on cDNA samples from the initial segment (IS) or caput epididymis of adult rats (PND90) subjected to sham procedure (control, CTL) or efferent ductules ligation (EDL) to study the modulation of *Pdi* transcripts by testicular factors. Data are mean ± SEM of experiments performed with samples from 3-6 rats per group. *Rpl19* was used as the reference gene. The average Cq value > 31 was used as a cutoff for low-expression transcripts (see Methods).

Transcripts	**Experimental Groups**			
	Initial segment (IS)		Caput	
	CTL	EDL	CTL	EDL
P4hb	21.59 ± 1.25	21.65 ± 1.28	21.82 ± 1.01	21.69 ± 1.43
Pdia3	21.50 ± 1.16	21.69 ± 1.32	22.02 ± 1.21	21.58 ± 1.75
Pdia5	23.68 ± 1.26	24.27 ± 1.37	24.12 ± 1.19	23.97 ± 1.50
Pdia6	17.57 ± 1.76	19.40 ± 0.75	19.20 ± 1.20	19.35 ± 1.67
Erp29	22.79 ± 0.97	22.82 ± 0.95	23.07 ± 0.81	22.96 ± 0.95
Pdilt	36.05 ± 1.61	36.50 ± 0.55	36.51 ± 1.13	35.37 ± 0.50
Rpl19	20.19 ± 0.91	20.28 ± 1.17	20.84 ± 0.77	20.14 ± 1.35

SUPPLEMENTAL TABLE S6. *Pdi* gene expression levels were assessed using NURSA transcriptome datasets, revealing insights into their transcriptional modulation within androgen receptor (AR) signaling pathways influenced by various regulatory molecules. These include AR agonists (T**,** testosterone; DHT, dihydrotestosterone; R1881, metribolone), the AR antagonist flutamide, siRNA against AR, estrogen receptor (ER) agonist (E2, 17β-estradiol), and AR co-modulators (HDAC1, histone deacetylase 1 in complex with other corepressors of AR gene expression). HDAC1 knockdown was observed to partially restore AR function, while. UTX (Ubiquitously Expressed Prefoldin Like Chaperone or AR trapped clone-27, ART-27) was found to enhance androgen-stimulated transcription. ELK1 (ETS Transcription Factor ELK1) was identified as non-essential for overall transcriptional activity of AR but crucial in AR-mediated growth signaling. *Pdi* genes were filtered based on a fold change (FC) criterion < -2 and > 2 ($p < 0.05$). Multiple entries for the same regulatory molecule within the same study account for different experimental conditions. The expression data, displayed as FC values, are presented. Consistent with our qPCR data, we found *Pdia5,* followed by *Pdia6*, *Erp29* and *Pdia3,* transcripts to be upregulated by androgens *in vitro* or by androgen receptor manipulation *in vivo*. The analysis also revealed that the *P4hb* mRNA is both up- and downregulated by androgens, whereas *Pdia2* transcript is downregulated by either agonists or antagonists of AR. The analysis sheds light on the intricate regulatory network controlling *Pdi* gene expression and its modulation within the AR signaling pathway.

AR Modulator		***Experimental Model***	***Pdi gene Expression Levels***						***References*****
			P4hb	***Pdia3***	***Pdia5***	***Pdia6***	***Erp29***	***Pdia2***	
Agonists	DHT	LNCaP Cells			2.04				Kazmin et al., 2006 [1]
		LNCaP Cells			2.54				Nickols and Dervan, 2007 [2]
		LNCaP Cells			2.36				Jia et al., 2008 [3]
		LNCaP Cells			3.83				Hieronymus et al., 2006 [4]
		LNCaP Cells			2.9				Massie et al., 2011 [5]
	R1881	LNCaP Cells			3.01				Nwachukwu et al., 2009 [6]
		LNCaP Cells + UTX knockdown			3.2				
		LNCaP Cells			4.69				Patik et al., 2013 [7]
		LNCaP Cells + ELK knockdown			4.08				
		LNCaP Cells + HDAC1 knockdown	2.31			2.44	2.09	-2.76	Welsbi et al., 2009 [8]
	T	Efferent Ductules	-2.08		6.04	8.38	8.83		Snyder et al., 2009 [9]
		Caput Epididymis		2.96	2.8	2.07		-2.19	
	T + E2	Caput Epididymis			2.69				
Antagonist	Flutamide	Whole lung (GD17.5) male x female						-6.98	Bresson et al., 2010 [10]
siRNA	AR-siRNA	LNCaP Cells			-2.02				He et al., 2014 [11]

***Method for Supplemental TABLE S6:** The Nuclear Receptor Signaling Atlas (NURSA), which is integrated with the Signaling Pathways Project (SPP; https://dknet.org), was used via the Transcriptomine tool (Ochsner et al. 2019). [12] This resource was used to extract publicly available transcriptomic datasets to gain insight into the mechanistic and functional roles of genes whose products interact with nuclear receptors. [13] Each *Pdi* gene was searched individually with default settings using the criteria of a significance level of $p \leq 0.05$ and a fold change threshold (FC) less than -2 and greater than 2 to identify examples of notable changes in gene expression. The FC values were treated in their unlogged form, indicating either induction/upregulation (FC >1) or repression/downregulation (FC < 1) of the respective transcript. The retrieved data were then acquired in .xlsx format and subjected to a manual filtering process that focused on the modulation of androgen receptor (AR) pathway. Each result was subjected to validation by querying the corresponding PubMed identification number (PMID) for authenticity. Data entries lacking an associated PMID or with a p-value of zero (either due to unavailability of the p-value by the author or lack of replicates within the datasets) were excluded.

****References cited in this Supplemental Table S6:**

1. Kazmin D, Prytkova T, Cook CE, et al. Linking ligand-induced alterations in androgen receptor structure to differential gene expression: A first step in the rational design of selective androgen receptor modulators. *Mol Endocrinol* . 2006;20(6):1201-1217. Doi:10.1210/me.2005-0309
2. Nickols NG, Dervan PB. Suppression of androgen receptor-mediated gene expression by a sequence-specific DNA-binding polyamide. *PNAS*. 2007;104(25):10418-10423. Doi:10.1073/pnas.0704217104.
3. Jia L, Berman BP, Jariwala U, et al. Genomic androgen receptor-occupied regions with different functions, defined by histone acetylation, coregulators and transcriptional capacity. *PLoS One*. 2008;3(11):e3645. Doi:10.1371/journal.pone.0003645
4. Hieronymus H, Lamb J, Ross KN, et al. Gene expression signature-based chemical genomic prediction identifies a novel class of HSP90 pathway modulators. *Cancer Cell*. 2006;10(4):321-330. Doi:10.1016/j.ccr.2006.09.005
5. Massie CE, Lynch A, Ramos-Montoya A, et al. The androgen receptor fuels prostate cancer by regulating central metabolism and biosynthesis. *EMBO J*. 2011;30(13):2719-2733. Doi:10.1038/emboj.2011.158
6. Nwachukwu JC, Mita P, Ruoff R, et al. Genome-wide impact of androgen receptor trapped clone-27 loss on androgen-regulated transcription in prostate cancer cells. *Cancer Res*. 2009;69(7):3140-3147. Doi:10.1158/0008-5472.CAN-08-3738
7. Patki M, Chari V, Sivakumaran S, Gonit M, Trumbly R, Ratnam M. The ETS domain transcription factor ELK1 directs a critical component of growth signaling by the androgen receptor in prostate cancer cells. *J Biol Chem*. 2013;288(16):11047-11065. Doi:10.1074/jbc.M112.438473

8. Welsbie DS, Xu J, Chen Y, et al. Histone deacetylases are required for androgen receptor function in hormone-sensitive and castrate-resistant prostate cancer. *Cancer Res*. 2009;69(3):958-966. Doi:10.1158/0008-5472.CAN-08-2216
9. Snyder EM, Small CL, Li Y, Griswold MD. Regulation of gene expression by estrogen and testosterone in the proximal mouse reproductive tract. *Biol Reprod*. 2009;81(4):707-716. Doi:10.1095/biolreprod.109.079053
10. Bresson E, Seaborn T, Côté M, et al. Gene expression profile of androgen modulated genes in the murine fetal developing lung. *Reprod Biol Endocrinol*. 2010;8(2). Doi:10.1186/1477-7827-8-2
11. He B, Lanz RB, Fiskus W, et al. GATA2 facilitates steroid receptor coactivator recruitment to the androgen receptor complex. *PNAS*. 2014;111(51):18261-18266. Doi:10.1073/pnas.1421415111
12. Ochsner SA, Abraham D, Martin K, et al. The Signaling Pathways Project, an integrated 'omics knowledgebase for mammalian cellular signaling pathways. *Sci Data*. 2019;6(252). Doi:10.1038/s41597-019-0193-4
13. Becnel LB, Darlington YF, Ochsner SA, et al. Nuclear receptor signaling atlas: Opening access to the biology of nuclear receptor signaling pathways. *PLoS One*. 2015;10(9):e0135615. Doi:10.1371/journal.pone.0135615